Phase transition in a U(1)-lattice-gauge system derived from a weakly three-dimensional t-J model

Yasuko Munehisa
Faculty of Engineering, Yamanashi University, Kofu, Yamanashi, 400 Japan
(Received 25 October 1991)

We numerically study a U(1)-lattice-gauge system, which is an effective model of the Ginzburg-Landau-type obtained from the t-J model of electrons. The model, which we call the "GL" model for short, is composed of link variables interpreted as a nearest-neighbor hole-pair field bounded by the singlet spin pairs. We concentrate our attention on the weakly three-dimensional case in which the electron hopping in the third direction is suppressed compared to other directions. When we simulate the model on an L^3 lattice, we therefore actually treat a system of L loosely coupled layers each of which is of size L^2. Monte Carlo simulations are done on 12^3, 20^3, and 30^3 lattices with the electron density slightly less than the half-filled one (the doping parameter δ is mostly 0.06) and with the ratio of the interlayer-to-intralayer hopping parameter ranging between 0.1 and 0.9. We observe cusplike behavior of the specific heat, which indicates a phase transition due to the spontaneous breaking of a global symmetry of the GL model. An average link variable in one direction within the layers turns out to serve as a nice order parameter of the transition. The transition temperature T_c decreases as the interlayer hopping of the electrons increases. Results on some expectation values, which indicate strong correlations between link variables below T_c, are also presented.

In the study of systems of strongly correlated electrons, the t-J model,[1] which originates from the Hubbard model with strong on-site Coulomb repulsion, is expected to shed light on the high-temperature superconducting phenomena. Several years ago it was pointed out in Refs. 2 and 3 that from the t-J model with small doping one can obtain a model of the Ginzburg-Landau-type (GL) model in terms of resonating valence bonds (RVB). This GL model, being constructed by a bounded scalar hole-pair field, may be categorized as a kind of U(1)-lattice-gauge-Higgs theory, although it is somewhat different from the conventional one studied in particle physics.[4] Since its form on a lattice is suitable for Monte Carlo simulations the GL model enables us to investigate the system beyond mean-field treatments. Numerical study along this line has been made by Nakamura and Matsui[3] on a square lattice with simplified version of the model, namely, with the amplitudes of the hole-pair field frozen to a mean-field value. Nakajima and Hori[5] also numerically studied the simplified model in two and weakly three dimensions including more interaction terms. In our previous study[6] we carried out simulations in two space dimensions taking full dynamical degrees of freedom of the model into account and found an outstanding peak in the specific heat, which we expect to be a precursor of a genuine transition that would emerge when a weak three dimensionality is included.

In this present work we show Monte Carlo results on the weakly three-dimensional GL model with full dynamical degrees of freedom.

Let us first briefly describe the model we study. We start from the t-J Hamiltonian

$$\hat{H}_{t\text{-}J}=-\sum_{i,\mu} t_\mu \hat{e}_i^\dagger \hat{a}_{i\pm\hat{\mu}}^\dagger \hat{a}_i \hat{e}_{i\pm\hat{\mu}} - \mu_c \sum_i (\hat{a}^\dagger \hat{a})_i + \sum_{i,\mu} \frac{J_\mu}{4} [(\hat{a}^\dagger \boldsymbol{\sigma} \hat{a})_i (\hat{a}^\dagger \boldsymbol{\sigma} \hat{a})_{i+\hat{\mu}} - (\hat{a}^\dagger \hat{a})_i (\hat{a}^\dagger \hat{a})_{i+\hat{\mu}}] , \tag{1}$$

which we expect keeps essentials of Hubbard Hamiltonian with strong Coulomb repulsion and small doping;

$$\hat{H}_{\text{Hubbard}}=-\sum_{i,\mu,\sigma} t_\mu \hat{C}_{i\sigma}^\dagger \hat{C}_{i\pm\hat{\mu},\sigma} + U \sum_i \hat{n}_{i1}\hat{n}_{i2} - \mu_c \sum_{i,\sigma} \hat{n}_{i\sigma} , \tag{2}$$

where the position index i runs all sites of three-dimensional lattice with unit lattice spacing, the direction index μ from 1 to 3, the spin index σ from 1 to 2 and $\hat{\mu}$ stands for unit vector in μ direction. In the Hamiltonian we denote annihilation operator of electron by $\hat{C}_{i\sigma}$ and the number operator $\hat{C}_{i\sigma}^\dagger \hat{C}_{i\sigma}$ by $\hat{n}_{i\sigma}$. Parameters t_μ, U, and μ_c represent nearest-neighbor hopping in μ direction, on-site Coulomb repulsion and chemical potential, respectively. In this work we always keep $t_1=t_2\equiv t$ and $0\le t_3<t\ll U$.

In the t-J Hamiltonian in (1) the antiferromagnetic coupling in the μ direction, J_μ, is defined as $J_\mu\equiv 4t_\mu^2/U$. As we assign $\hat{e}_i^\dagger$ to a canonical boson operator, which creates the charged hole state, and $\hat{a}_{i\sigma}^\dagger$ to a canonical fermion operator to create the neutral spin state, the electron operator $\hat{C}_{i\sigma}$ in (2) is expressed as $\hat{e}_i^\dagger \hat{a}_{i\sigma}$. (Here we neglect double occupancy.) Having integrated over fermion fields in the same manner as in Ref. 6 we obtain the

path-integral expression of the partition function $Z=\mathrm{Tr}\{\exp(-\beta\hat{H})\}$ of the GL model with nearest-neighbor interactions between complex link variables $M_{i\mu}\equiv\rho_{i\mu}\cdot e^{i\theta_{i\mu}}$, which represents a charge $2e$ hole-pair field divided by the doping parameter δ:

$$
\begin{aligned}
&Z=\int [dM_{i\mu}]\exp(A_{\mathrm{GL}})\ , \quad A_{\mathrm{GL}}=A_0+A_M\ ,\\
&A_0=2\beta\mu_c V(1-\delta)+2\sum_p \ln\left\{1+\exp\left[\beta\left[2\delta\sum_\mu t_\mu\cos p_\mu-\mu_c\right]\right]\right\}\ ,\\
&A_M=\sum_{i,\mu} c_{2\mu}\overline{M}_{i\mu}M_{i\mu}+\Bigg\{\sum_{i,\mu\neq\nu}\sigma_{1\mu\nu}\overline{M}_{i+\hat{\nu},\mu}M_{i\mu}+\sum_{i,\mu}\sigma_{2\mu}\overline{M}_{i\mu}M_{i-\hat{\mu},\mu}\\
&\qquad\qquad+\sum_{i,\mu<\nu}\sigma_{3\mu\nu}(\overline{M}_{i\mu}M_{i-\hat{\nu},\nu}+\overline{M}_{i-\hat{\mu},\mu}M_{i-\hat{\nu},\nu}+\overline{M}_{i\mu}M_{i\nu}+\overline{M}_{i-\hat{\mu},\mu}M_{i\nu})+\mathrm{c.c.}\Bigg\}\\
&\quad-\sum_{i,\mu}\lambda_{\mu\mu}(\tfrac{1}{2}\rho_{i\mu}^4+\rho_{i-\hat{\mu},\mu}^2\rho_{i\mu}^2)-\sum_{i,\mu<\nu}\lambda_{\mu\nu}(\rho_{i\mu}^2\rho_{i\nu}^2+\rho_{i-\hat{\mu},\mu}^2\rho_{i\nu}^2+\rho_{i\mu}^2\rho_{i-\hat{\nu},\nu}^2+\rho_{i-\hat{\mu},\mu}^2\rho_{i-\hat{\nu},\nu}^2)\\
&\quad-\sum_{i,\mu<\nu}\lambda_{\mu\nu}(M_{i\mu}\overline{M}_{i+\hat{\mu},\nu}M_{i+\hat{\nu},\mu}\overline{M}_{i\nu}+\mathrm{c.c.})\ ,
\end{aligned}
\tag{3}
$$

where β is the inverse temperature ($\beta\equiv 1/k_BT$ with temperature T and the Boltzmann constant k_B), $V\equiv L^3$ is the number of lattice sites, and $\overline{M}_{i\mu}$ denotes a complex conjugate of $M_{i\mu}$. It should be noted that both radial and phase degrees of freedom of $M_{i\mu}$ are active.

The GL coefficients

$$
\begin{aligned}
&c_{2\mu}=J_\mu(G_{00}+G_{\mu\mu})-\beta\ ,\\
&\sigma_{1\mu\nu}=J_\mu G_{\nu\nu}\ ,\\
&\sigma_{2\mu}=J_\mu(G_{\mu\mu}+G_{0,\mu+\mu})\ ,\\
&\sigma_{3\mu\nu}=\sqrt{J_\mu J_\nu}(G_{\mu\nu}+G_{0,\mu+\nu})\ ,\\
&\lambda_{\mu\nu}=\tfrac{1}{2}J_\mu J_\nu G_{44}
\end{aligned}
\tag{4}
$$

are defined in terms of the thermal Green's functions G_{jl} given by

$$
\begin{aligned}
&G_{00}=\sum_n g_n(0)g_n(0)^*\ ,\\
&G_{\mu\nu}=\tfrac{1}{2}\sum_n[g_n(\hat{\mu})g_n(\hat{\nu})^*+g_n(\hat{\mu})^*g_n(\hat{\nu})]\ ,\\
&G_{0,\mu+\nu}=\tfrac{1}{2}\sum_n[g_n(0)g_n(\hat{\mu}+\hat{\nu})^*+g_n(0)^*g_n(\hat{\mu}+\hat{\nu})]\ ,\\
&G_{44}=\sum_n[g_n(0)g_n(0)^*]^2\ ,
\end{aligned}
\tag{5}
$$

where

$$
\begin{aligned}
&g_n(x)=\frac{\Delta\beta}{V}\sum_k\frac{\exp(ipx)}{\exp(i\omega_n)-1-\Delta\beta[2\delta\sum_\mu t_\mu\cos p_\mu-\mu_c]}\ ,\\
&\omega_n=\frac{(2n-1)\pi}{N}\quad(n=1,2,\ldots,N)\ ,\quad \Delta\beta=\frac{\beta}{N}\ ,\\
&p_\mu\equiv\frac{2\pi k_\mu}{K}\quad(k_\mu=1,\ldots,K)\ .
\end{aligned}
\tag{6}
$$

As some of the GL coefficients become equal by definition we actually have twelve different coefficients for positive δ and t_3 between 0 and t. They are $c_{2x}\equiv c_{2,1}=c_{2,2}$, $c_{2z}\equiv c_{2,3}$, $\sigma_{1xy}\equiv\sigma_{1,12}=\sigma_{1,21}$, $\sigma_{1xz}\equiv\sigma_{1,13}=\sigma_{1,23}$, $\sigma_{1zx}\equiv\sigma_{1,31}=\sigma_{1,32}$, $\sigma_{2x}\equiv\sigma_{2,1}=\sigma_{2,2}$, $\sigma_{2z}\equiv\sigma_{2,3}$, $\sigma_{3xy}\equiv\sigma_{3,12}$, $\sigma_{3xz}\equiv\sigma_{3,13}=\sigma_{3,23}$, $\lambda_{xx}\equiv\lambda_{11}=\lambda_{22}=\lambda_{12}$, $\lambda_{xz}\equiv\lambda_{13}=\lambda_{23}$, and $\lambda_{zz}\equiv\lambda_{33}$.

When $t_3=0$ the action in (3) reduces to the two-dimensional one[6] except for an extra term $-\beta\sum_i\rho_{i3}^2$. This extra term decouples from the rest of the action in the partition function so that the model essentially describes two-dimensional physics. If we set $t_3=t$ we obtain (symmetric) three-dimensional GL action.

For any t_3 the GL action is locally gauge invariant when $\delta=0$ (half filled), for which all σ_1's, σ_2's, and σ_3's vanish, while for positive δ it is invariant only under global gauge transformation

$$
M_{i\mu}\rightarrow e^{i\alpha}M_{i\mu}\ . \tag{7}
$$

In Monte Carlo simulations using a Metropolis algorithm we measured the number of electrons N, internal energy E, and specific heat C_v:

$$
\begin{aligned}
&N=\frac{1}{\beta}\frac{\partial}{\partial\mu_c}\ln Z\ ,\\
&E=-\frac{\partial}{\partial\beta}\ln Z+\mu_c N\ ,\\
&C_v=\frac{dE}{dT}=-k\beta^2\frac{dE}{d\beta}=-k\beta^2\left[\frac{\partial}{\partial\beta}+\frac{\partial\mu_c}{\partial\beta}\frac{\partial}{\partial\mu_c}\right]E\ .
\end{aligned}
\tag{8}
$$

We also measured average links in each direction

$$
M_\mu\equiv\left\langle\frac{1}{V}\sum_i M_{i\mu}\right\rangle\ , \tag{9}
$$

where $\langle\ \rangle$ stands for the ensemble average, average squared amplitudes

$$
\rho_\mu^2\equiv\left\langle\frac{1}{V}\sum_i\rho_{i\mu}^2\right\rangle\ , \tag{10}
$$

average bond-hopping terms

$$H_{1\mu\nu}\equiv \mathrm{Re}\left\langle \frac{1}{V}\sum_i \overline{M}_{i+\hat{\nu},\mu}M_{i\mu}\right\rangle ,$$

$$H_{2\mu}\equiv \mathrm{Re}\left\langle \frac{1}{V}\sum_i \overline{M}_{i\mu}M_{i-\hat{\mu},\mu}\right\rangle ,$$

$$H_{3\mu\nu}\equiv \mathrm{Re}\left\langle \frac{1}{4V}\sum_i (\overline{M}_{i\mu}M_{i-\hat{\nu},\nu}+\overline{M}_{i-\hat{\mu},\mu}M_{i-\hat{\nu},\nu} +\overline{M}_{i\mu}M_{i\nu}+\overline{M}_{i-\hat{\mu},\mu}M_{\nu})\right\rangle , \quad (11)$$

and average plaquettes including (excluding) radial degrees of freedom

$$P_{\mu\nu}\equiv \mathrm{Re}\left\langle \frac{1}{V}\sum_i M_{i\mu}\overline{M}_{i+\hat{\mu},\nu}M_{i+\hat{\nu},\mu}\overline{M}_{i\nu}\right\rangle ,$$

$$\theta_{p\mu\nu}\equiv \left\langle \frac{1}{V}\sum_i \cos(\theta_{i\mu}-\theta_{i+\hat{\mu},\nu}+\theta_{i+\hat{\nu},\mu}-\theta_{i\nu})\right\rangle . \quad (12)$$

In a previous work we learned that Monte Carlo results depend much on the value of the doping parameter δ. In this work we make most numerical studies at $\delta=0.06$ for which a mild peak of the specific heat has been observed at $T\simeq 40$ K in the two-dimensional case.[6] Some simulations are also carried out at $\delta=0.04$ and 0.08 for comparison. Fixing $U=3.6$ eV and $t=0.3$ eV throughout this work, we widely change the ratio $r\equiv t_3/t$ between 0 and 1 so that we can examine relations between weakly three-dimensional features and two- or three-dimensional ones. We also made several simulations with $r=0$ to ensure that present model reproduces two-dimensional results. Simulations with $r=1$ could not been performed for technical reasons stated below.

We find that some of the GL coefficients and their derivatives, especially μ_c derivatives, are quite sensitive to the lattice size used to calculate them. This may bring serious size dependence of the adjusted chemical potential, which is numerically determined so that the measured average electron density N/V equals $1-\delta$ within 1% accuracy. We therefore calculate the chemical potential and the GL coefficients on K^3 lattices with $K\geq 30$ to obtain stable values.

Using these coefficients Monte Carlo simulations of the system are then performed on an L^3 lattice with periodic boundary conditions, where we mostly use the $L=12$ lattice. We also carried out some simulations on $L=20$ and 30 lattices to examine finite-size effects. On each lattice typically 1000 sweeps with six hits at every sweep are done for the thermalization and 10000 configurations after the thermalization divided into ten bins are used for the measurement. Statistical errors are estimated by the deviation among those bins.

Now we present our results. We made measurements on 12^3, 20^3, and 30^3 lattices for $\delta=0.06$ and $r=0.5$ and 0.1. For either r we did not observe any serious size dependence of the data. Other measurements are done on a 12^3 lattice.

In Fig. 1 specific heat per unit volume (with unit lattice spacing), $c_v\equiv C_v/V$, with $\delta=0.06$ is plotted as a function of T for several values of r. We see for each r the specific heat has a maximum, whose location shifts toward lower

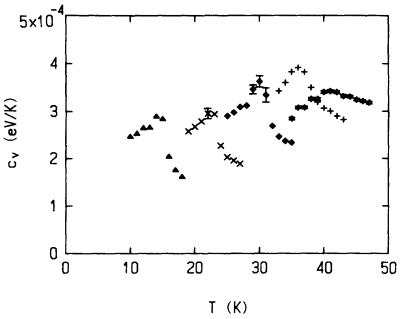

FIG. 1. Specific heat per unit volume (with unit lattice spacing) with $\delta=0.06$ vs temperature. Asterisks are data for $r=0.1$, plusses for $r=0.3$, squares for $r=0.5$, crosses for $r=0.7$, and triangles for $r=0.9$. Data for $r=0.1$ and 0.5 are measured on a 20^3 lattice, while other data are measured on a 12^3 lattice. Statistical errors of are within marks if not shown explicitly.

T as r increases. Location of the maximum with $r=0.1$ is almost the same as two-dimensional one.[6] The value of the maximum increases when we change $r=0.1$ to 0.3 and then becomes smaller for larger r. Shape of the specific-heat curve is cusplike for $r\geq 0.3$, while a mild bump is observed for $r=0.1$.

Figure 2 shows the absolute value of the average link in $\mu=1$ direction, $|M_1|$, versus T on a 30^3 lattice with $r=0.1$ and 0.5. The results clearly prove this quantity nicely serves as an order parameter of the phase transition. Above the transition temperature, T_c, $|M_1|$ is consistent with zero, while below T_c it rapidly becomes finite. One can see such behavior of $|M_1|$ even on a 12^3 lattice, but measurements on a large lattice are needed to decide T_c with satisfying accuracy. From results in Figs. 1 and 2 we see the location of the specific-heat maximum is only slightly lower than T_c for $r=0.5$, while the former is much greater than the latter when $r=0.1$.

Data on $|M_1|$ with $r=0.3$, 0.7, and 0.9 measured on a 12^3 lattice are all similar to those with $r=0.5$. For $r\geq 0.3$, therefore, we can say that a drastic change of specific heat as well as $|M_1|$ signals the occurrence of the transition. For all r we also observe that $|M_2|=|M_1|$ and

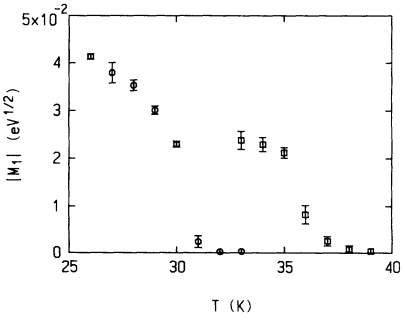

FIG. 2. Absolute value of the average link in $\mu=1$ direction for $\delta=0.06$ on a 30^3 lattice as a function of temperature. Circles are data for $r=0.5$ and squares are for $r=0.1$. Statistical errors are within circles or squares if not shown explicitly.

$|M_3| \simeq 0$ within errors. One unexpected result we find is that $|M_1 + M_2| = 0$ holds to quite good accuracy for any r and any T.

In Figs. 3(a), 3(b), and 3(c) we plot several expectation values measured in simulations with $r = 0.5$ and $\delta = 0.06$. Figure 3(a) presents average squared amplitude ρ_1^2 and ρ_3^2 versus T. We see data on ρ_3^2 are in good agreement with straight line $k_B T$. This indicates that amplitudes in the $\mu = 3$ direction scarcely correlate with each others as they do in the high-T limit.[6] On the other hand ρ_1^2 (as well as ρ_2^2) shows kinklike behavior, which is almost constant below T_c and rises linearly above T_c. These results suggest it would not be appropriate to fix the amplitude of $M_{i\mu}$ by its mean-field value.

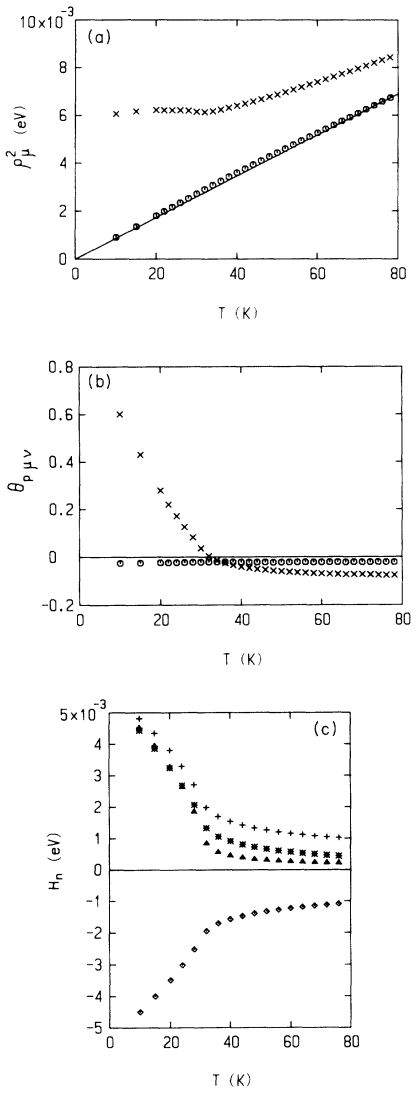

FIG. 3. Expectation values on a 12^3 lattice measured for $\delta = 0.06$ and $r = 0.5$. Statistical errors are within the marks. (a) Average squared amplitude in the $\mu = 1$ direction (crosses) and $\mu = 3$ direction (circles) with straight line representing $k_B T$. (b) Average plaquette excluding radial degrees of freedom. Crosses are data in the ($\mu = 1$, $\nu = 2$) plane and circles in the ($\mu = 1$, $\nu = 3$) plane. (c) Parallel bond hopping terms within and across layers $H_{1,12}$ (plusses) and $H_{1,13}$ (triangles), the collinear bond-hopping term $H_{2,1}$ (asterisks), and the perpendicular bond-hopping term $H_{3,12}$ (squares).

Figure 3(b) plots average plaquette without radial degrees of freedom, $\theta_{p\mu\nu}$, defined in (12). The results show θ_{p12}, namely, θ_p in the layer, rapidly increase below T_c and has positive values in spite of the fact that they are not energetically favored. [Note that all λ's are positive by definition in (4) and (5).] Across layers, on the other hand, θ_{p13} (as well as θ_{p23}) scarcely depends on temperature, having small but finite negative values.

In Fig. 3(c) we show some average bond-hopping terms whose value we observe to be nonzero, namely $H_{1,12}$, $H_{1,13}$, $H_{2,1}$, and $H_{3,12}$ defined in (11). We see $H_{3,12}$ is negative and rapidly decreases when T goes down across T_c, while other terms are all positive and rapidly increase below T_c. We also observe $H_{1,21} \simeq H_{1,12}$, $H_{1,23} \simeq H_{1,13}$, and $H_{2,2} \simeq H_{2,1}$ as expected.

Results in Figs. 2 and 3 indicate that phases of link variables strongly correlate in some special manner at low temperatures. This will be discussed later.

So far we have presented results for $\delta = 0.06$ with various values of r. Now we comment on some results for $\delta = 0.04$ and 0.08 with $r = 0.5$ on a 12^3 lattice. In the previous study[6] in two dimensions we observed a sharp peak of the specific-heat for $\delta = 0.04$, while data for $\delta = 0.08$ showed a kink only. In contrast to these two-dimensional results, the shape of the specific heat with $r = 0.5$ does not drastically change for δ's we study. We see cusplike behavior even for $\delta = 0.08$, the maximum values of the cusp mildly decreasing as δ increases from 0.04 to 0.08. The transition temperature estimated from $|M_1|$ data with $\delta = 0.04$ is lower by ~ 5 K than T_c for $\delta = 0.06$, while T_c for $\delta = 0.08$ is only slightly lower than T_c for $\delta = 0.06$. These results suggest the maximum value of T_c would be observed for some δ between 0.06 and 0.08.

In the weakly three-dimensional GL model studied we have observed several interesting features. Remarks on them are now in order.

First, results on the $|M_\mu|$'s indicate that the global symmetry of the GL action (3) spontaneously breaks in $\mu = 1$ and 2 directions. Since such a breakdown is known to be impossible in two-dimensions (Mermin's theorem), the dimensionality of the model proves to play a very important role in this transition even when electron hopping across layers is discouraged. Physically, the fact that $|M_\mu|$ is finite signals hole-pair condensation below the transition temperature. Another observation that $|M_1 + M_2| = 0$ holds with good accuracy would mean the wave function is of the d-wave type. This is an intriguing mechanism of phase transition in the GL model, as clarified in this study. Whether such a transition really takes place in some material is, however, not clear yet and should be examined in a future study.

The second feature we would like to comment on is the location of the transition temperature T_c. Figure 1 roughly shows how T_c for $\delta = 0.06$ depends on r, since the specific heat maximizes near T_c, as we have mentioned above. We see that T_c *decreases* as r grows so that the phase transition in three dimensions (namely, for $r = 1$), if any, would take place in a region below 10 K,

which is too low to study by our present techniques of numerical calculation. It is a somewhat unexpected observation that T_c becomes lower as coupling between the layers strengthens. This is in contrast to the results on the XY model,[7] for which T_c is reported to increase in the same situation.

As we have shown in Fig. 1 specific heat with $r=0.1$ forms a mild bump that resembles the two-dimensional result[6] rather than cusps as observed for $r \geq 0.3$, in spite of the fact that $|M_1|$ behaves similarly for all r. It is not yet clear what makes such differences nor whether essential differences exist between the system with $r \geq 0.3$ and the system with $r=0.1$. Further study will be necessary on this point.

Finally let us discuss, based on results in Figs. 2 and 3, what configurations prevail below T_c. Results on ρ_μ^2 in Fig. 3(a) suggest that not the radial degrees of freedom but the phase degrees of freedom are responsible for spontaneous symmetry breaking shown in Fig. 2. Results on average plaquette and bond hopping terms in figs. 3(b) and 3(c) indicate when the system is cool enough several terms with coefficients σ_1, σ_2, and σ_3 dominate in the GL action so that the phase degrees of freedom strongly correlate in favor of these terms. Namely, θ_{i1}'s (θ_{i2}'s) in each layer tend to align to make $H_{1,12}$ and $H_{2,1}$ ($H_{1,21}$ and $H_{2,2}$) positive for positive coefficients σ_{1xy} and σ_{2x}. Perpendicular bond-hopping terms $H_{3,12}$, on the other hand, are observed to be negative as energetically favored because of the negativeness of σ_{3xy}. This is realized by θ_{i2}'s mostly antiparallel to θ_{i1}'s. Positive coefficient σ_{1xz} then plays an essential role to bring spontaneous symmetry breaking by aligning θ_{i1}'s (θ_{i2}'s) across layers. Direct scans we made over some typical configurations support this picture.

In this work we studied cases with $r \geq 0.1$. If this GL model has something to do with high-T_c superconducting mechanism, cases with very small r would be realistic and important. Much larger lattices will be necessary, however, to observe spontaneous symmetry breaking in such cases.

ACKNOWLEDGMENTS

The author is thankful to Tomo Munehisa for very valuable discussions and much encouragement. The numerical calculations have been carried out on the HITAC S820 at the University of Tokyo.

[1]P. W. Anderson, Science **235**, 1196 (1987); G. Baskaran, Z. Zou, and P. W. Anderson, Solid State Commun. **63**, 973 (1987); A. E. Ruckenstein, P. J. Hirschfeld, and J. Appel, Phys. Rev. B **36**, 857 (1987).

[2]G. Baskaran and P. W. Anderson, Phys. Rev. B **37**, 580 (1988).

[3]A. Nakamura and T. Matsui, Phys. Rev. B **37**, 7940 (1988).

[4]Y. Munehisa, Phys. Lett. **155B**, 159 (1985); K. Jansen, J. Jersák, C. B. Lang, T. Neuhaus, and G. Vones, Nucl. Phys. **B265**, [FS15], 129 (1986), and references cited therein.

[5]H. Nakajima and Y. Hori, Phys. Rev. B **43**, 480 (1991).

[6]Y. Munehisa and T. Matsui, Phys. Rev. B **43**, 11 388 (1991).

[7]W. Janke and T. Matusi, Phys. Rev. B **42**, 10 673 (1990).